CNWRA *A center of excellence in earth sciences and engineering*

A Division of Southwest Research Institute™
6220 Culebra Road • San Antonio, Texas, U.S.A. 78228-5166
(210) 522-5160 • Fax (210) 522-5155

July 18, 2001
Contract No. NRC-02-97-009
Account No. 20.01402.571

U.S. Nuclear Regulatory Commission
ATTN: Mrs. Deborah A. DeMarco
Two White Flint North
11545 Rockville Pike
Mail Stop T8 A23
Washington, DC 20555

Subject:Programmatic review of a paper

Dear Mrs. DeMarco:

The enclosed paper is being submitted for programmatic review. The paper will be submitted for presentation at the 10th International Conference on Environment Degradation of Materials in Nuclear Power Systems—Waster Reactors to be held August 5–9, 2001 in Lake Tahoe, Nevada. The title of this paper is:

"General and Localized Corrosion of Zircaloy Under High-Level Radioactive Waste Disposal Conditions" by G. A. Cragnolino, C.S. Brossia, and D.S. Dunn.

This paper is a result of the activities conducted in FY2000 and FY2001 under task 01402.571 to resolve the issue related to the effects of engineering materials on the chemistry of water.

Sincerely,

Budhi Sagar
Technical Director

Enclosure

BS:VJ:jg

cc:	J. Linehan	J. Greeves	T. Ahn	J. Thomas	CNWRA EMs	P. Maldonado
	J. Piccone	C. Greene	T. Essig	G. Cragnolino		T. Nagy (contracts)
	B. Meehan	K. Stablein	T. Bloomer	W. Patrick	D. Dunn	
	E. Whitt	B. Leslie	J. Andersen	CNWRA Dirs.	S. Brossia	

Washington Office • Twinbrook Metro Plaza #210
12300 Twinbrook Parkway • Rockville, Maryland 20852-1606

General and Localized Corrosion of Zircaloy Under High-Level Radioactive Waste Disposal Conditions

G. A. Cragnolino, C. S. Brossia, D. S. Dunn
Center for Nuclear Waste Regulatory Analyses
Southwest Research Institute
6220 Culebra Road
San Antonio, TX 78238-5166

C. A. Greene
US Nuclear Regulatory Commission
Washington, DC 20555-0001

Abstract

Zircaloy (-2 and -4) spent nuclear fuel cladding is considered by the U. S. Department of Energy as an additional metallic barrier for the containment of radionuclides in the proposed repository at Yucca Mountain, Nevada. The general and localized corrosion of Zircaloy cladding under disposal conditions is discussed on the basis of literature data and our own investigations conducted in chloride-containing solutions which include anions present in the groundwater and simulate possible aqueous environments inside breached waste packages. These environments encompass a wide range of temperatures (25 to 95 °C), chloride concentrations (0.001 to 4.0 M), and pHs (2.1 to 10.7). The behavior of Zircaloy is evaluated using specimens covered with hydrothermally grown oxide films in comparison to freshly polished specimens. Ranges of passivity and localized corrosion, including critical potentials, are determined and studied using cyclic potentiodynamic and potentiostatic polarization tests. Corrosion potential measurements are conducted to follow the evolution of the potential with time and the occurrence of localized corrosion under naturally corroding conditions in the presence of oxidizing species such as iron (III) cations and hydrogen peroxide that could be present in the in-package environment.

Introduction

A large portion of the commercial spent nuclear fuel to be disposed in the proposed repository at Yucca Mountain, Nevada, is clad with Zircaloy-2 (Zr-2)[(1)] or Zircaloy-4 (Zr-4)[(2)]. These two Zr-1.5%Sn alloys contain Fe, Cr, and Ni as minor alloying elements but differ in the Ni content that is much lower in Zr-4 to decrease the hydrogen pick-up as a result of corrosion in high temperature water. U.S. Department of Energy (DOE), in its performance assessment of the proposed repository, has assumed that Zr-2 or Zr-4 cladding can be an additional metallic barrier to radionuclide release.[1]

Zr alloys, and in particular Zr-2 and Zr-4, exhibit exceptional corrosion resistance in a variety of aqueous solutions over a wide range of pHs and temperatures due to the formation of a protective passive film composed of ZrO_2. However, Zr and its alloys are known to be susceptible to various degradation modes as a result of aqueous corrosion that may lead to the failure of fuel cladding under disposal conditions, including general corrosion, localized corrosion, and stress corrosion cracking. The general aqueous corrosion of Zr-2 and Zr-4 at temperatures up to 300°C has been extensively investigated.[2,3] The protective oxide film growth rate is initially dependent on $(\text{time})^{-2/3}$, but undergoes a transition to a higher, approximately linear rate after some period of time. The oxide film in the spent nuclear fuel cladding typically has a thickness which increases with average rod burnup, ranging from 10 to 60 μm as a result of oxidation during the fuel cycle under reactor operating conditions.[3] Breakdown of the oxide film formed under service conditions, followed

[1]UNS R60802.

[2]UNS R60804.

by the initiation and propagation of localized corrosion can significantly shorten the life of the nuclear fuel cladding under repository conditions.

Of the species expected to be present in the groundwater at Yucca Mountain, chloride and fluoride anions are considered to likely have the most significant effect on localized corrosion of Zr- 2 or Zr-4. We have conducted an extensive review of the existing literature on the general and localized corrosion of Zr and its alloys.[4] It was concluded from this review that pitting corrosion occurs in both neutral and acidic chloride solutions above a critical potential for pitting initiation, which decreases linearly with the logarithm of the chloride concentration. The breakdown potential measured by potentiodynamic polarization methods is not only dependent on the potential scan rate and surface preparation but it is also affected by the stochastic nature of pit initiation. However, the pitting potential measured by galvanostatic methods or potentiostatic techniques combined with mechanical disruption of the passive film by straining and scratching is very reproducible and coincides with the repassivation potential, E_{rp}, measured by slow, backward potential stepping or scanning once pitting corrosion has initiated. E_{rp}, also follows a linear logarithmic dependence on the chloride concentration similar to the well established expression for the pitting initiation potential found for other metals and alloys.[5]

The purpose of this investigation is to examine the uniform and localized (pitting and crevice) corrosion behavior of Zr-4 under environmental conditions simulating those that may develop inside breached waste packages for spent nuclear fuel. In a previous paper[6], we have reported the behavior of mechanically polished specimens exposed to simulated groundwater containing chloride ions and covering a wide range of chloride concentrations. We found that pitting corrosion occurred on the boldly exposed surface of the specimens in cyclic potentiodynamic polarization tests but no crevice corrosion was detected. A limited set of experiments was conducted with specimens covered with an oxide layer thermally grown in air at 200 °C. It was found that E_{rp} was almost independent of the presence of the thermally grown oxide, but the morphology of the localized attack changed substantially from a network of shallow pits to isolated and deep, hemispherical pits. In this paper, the study is extended to specimens covered with thicker, hydrothermally grown oxide films. Because iron (III) cations can be present inside breached containers as a result of the corrosion of internal steel components and H_2O_2 can be generated as a stable product of the γ-radiolysis of water, the effect of these oxidizing species on the evolution of the corrosion potential and the occurrence of pitting corrosion was also evaluated on oxide covered specimens.

Experimental Procedures

All tests were performed using a single heat of Zr-4, whose chemical composition is shown in Table 1. Specimens were machined from an annealed 9.5 mm thick plate either in the form of cylinders 6.3 mm in diameter and 48.6 mm in length or as standard crevice specimens. Creviced specimens were constructed by pressing, with a torque of 0.35 N·m, a serrated polytetrafluoroethylene (PTFE) crevice former against a 1.9 × 1.9 × 1.3 cm (length × width × thickness) block. The specimens were wet polished to a 600 grit finish prior to testing. For creviced specimens, the crevice was loosely assembled in air and then fully tightened inside the solution. Some cylindrical specimens were oxidized in deionized (DI) water inside an autoclave at 300 °C for periods of 2, 4, 8, and 12 weeks to study the effect of the oxide layer thickness on the corrosion behavior of Zr-4. Based on the weight gain, and using the relationship provided by Hillner et al.,[7] approximate oxide thicknesses for the various exposure periods were calculated and listed in Table 2.

Table 1. Composition of Zr-4 Utilized in Current Study (in wt %)

Sn	Fe	Cr	Ni	O (ppm)	Zr
1.51	0.20	0.10	0.0035	1420	bal.

Initial tests were performed in chloride solutions containing 0.25 mM sulfate (SO_4^{2-}), 0.16 mM nitrate (NO_3^-), 0.10 mM fluoride (F^-) and a total carbonate ($HCO_3^- + CO_3^{2-}$) concentration of 1.4 mM, in order to simulate the chemical composition of the groundwater in the vicinity of Yucca Mountain as represented by J-13 well water. The presence of these additional anions, however, was shown to have only a minimal effect on the corrosion behavior of

Table 2. Weight Gain and Resulting Oxide Thickness During Hydrothermal Oxidation of Zr-4. Thickness Calculated from Weight Change Using Relationship Provided by Hillner et al.[7]

Exposure Time (weeks)	Weight Gain (mg)	Weight Gain/Unit Area (mg/dm^2)	Thickness (μm)
2	2.06	25.12	1.7
4	3.28	40.01	2.7
8	3.87	47.19	3.2
12	4.16	50.68	3.4

Zr-4 in the presence of chloride concentrations above 1 mM and thus were excluded from further use.[6] The chloride concentrations examined ranged from 1mM to 4M. In some experiments conducted in 0.1 M chloride solution, the concentration of fluoride was increased to 0.5 and 10 mM. All solutions were prepared using reagent grade sodium salts and 18 MΩ·cm water. The tests were conducted at three temperatures, 25, 65, and 95 °C. The solution was purged with high purity N_2 and heated to the desired temperature. The specimen was then introduced into the cell and the test was initiated after measuring the initial rest potential.

Both cyclic potentiodynamic polarization (CPP) and potentiostatic tests were performed to examine the conditions under which localized corrosion of Zr-4 takes place. All tests were conducted using a saturated calomel reference electrode (SCE) maintained at room temperature and connected to the cell through a salt bridge/Luggin probe filled with either 100 mM or 1 M chloride solution depending on the concentration of the testing solution. A platinum foil was used as a counter electrode. CPP tests were initiated at 0.1 V less than the open circuit potential after the specimen had been immersed in solution for an adequate period of time such that a steady state corrosion potential, E_{corr}, was reached. A potential scan rate of 0.167 mV/s was used and the scans were reversed when a current density of 5 mA/cm^2 was reached.

A series of open circuit potential measurements were also conducted to examine the possibility of exceeding the critical potentials for localized corrosion under naturally corroding conditions. These tests were performed in air-saturated solutions, in which synthetic (CO_2-free) air was purged continuously into the cell. The tests also involved, after a steady potential was reached, the addition of hydrogen peroxide and ferric chloride to enhance the oxidizing power of the solution.

Results

Figure 1 shows a typical CPP curve for a mechanically polished Zr-4 specimen in deaerated 0.1M NaCl at 95 °C. A breakdown potential, E_b, of about 0.20 V_{SCE} and a repassivation potential, E_{rp}, of about 0.10 V_{SCE} are clearly noticeable in the CPP curve, in addition to a wide passive range that extends over almost 1 V above the corrosion potential, which is approximately −0.7 V_{SCE} in the deaerated solution. For comparison, the CPP curve obtained with a specimen covered with a hydrothermally formed oxide film of about 3.2 μm in thickness is also shown in Figure 1. In this case, E_b is equal to 0.75 V_{SCE}, which is significantly higher than that measured in the polished specimen, whereas the value of E_{rp} is practically identical for both types of specimens. As expected, E_{corr} was found to be significantly higher (by about 0.5 V) for the specimen covered with the hydrothermally grown oxide.

The values of E_b for the mechanically polished specimens in the deaerated simulated J-13 well water (pH 8.4) are plotted in Figure 2 as a function of the chloride concentration for the three temperatures studied. As previously reported,[6] there was little variation of E_b for any given chloride concentration over the temperature range of 25 to 95 °C. All the data for tests in solutions with chloride concentrations ranging from 0.01 M to 4 M fit a linear logarithmic relationship independent of temperature given by

$$E_b = E_b^0 - B\log[Cl^-] \quad (1)$$

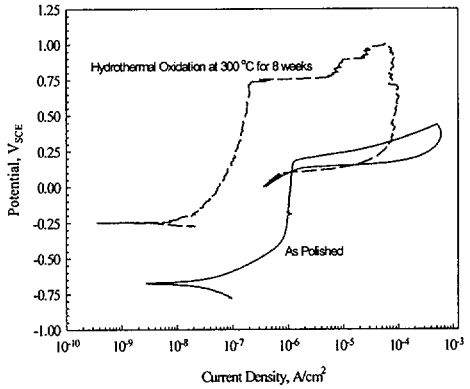

Figure 1. Cyclic potentiodynamic polarization curves for mechanically polished and hydrothermal oxide covered specimens of Zircaloy-4 in deaerated 0.1 M NaCl solution at 95 °C using a scan rate of 0.167 mV/s

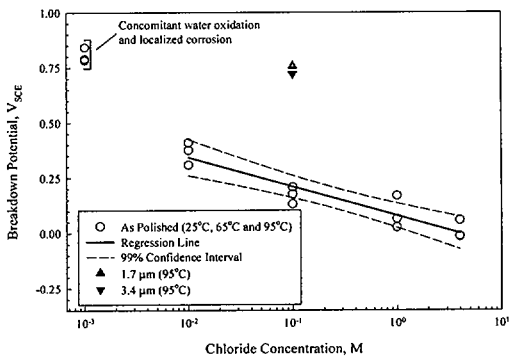

Figure 2. Breakdown potentials as a function of chloride concentration for mechanically polished specimens of Zircaloy-4 in simulated J-13 well water compared to values obtained for specimens covered with a hydrothermally grown oxide

where B and $E_b°$ were found to be equal to 131 mV/decade and 0.08 V_{SCE} respectively. At a chloride concentration of 0.001 M (1mM), however, E_b was found to be very high exhibiting a significant deviation of the linear dependence on the logarithm of the chloride concentration. This deviation is undoubtedly associated with the concomitant oxidation of water and the evolution of oxygen. In the same figure, the high E_b values obtained for hydrothermally oxidized specimens (2 and 8 weeks at 300 °C) in 0.1 M chloride solutions at 95 °C are included for comparison.

As shown in Figure 3, the plot of E_{rp} as a function of chloride concentration for the polished specimens in tests conducted in the simulated J-13 water (pH 8.4) exhibits a similar independence of temperature as that observed for E_b in Figure 2.[6] Also, E_{rp} displayed a linear logarithmic dependence on chloride concentration, given by

$$E_{rp} = E^0_{rp} - B\log[Cl^-] \quad (2)$$

but the linear dependence extends to the lowest chloride concentration. The temperature-independent values of B and $E°_{rp}$ are both lower than those for the passivity breakdown relationship and equal to 83 mV/decade and 0.04 V_{SCE} respectively. The most important observation, however, is that E_{rp} in 0.1 M chloride solutions at 95 °C for both hydrothermally oxidized specimens (2 and 8 weeks at 300 °C) is almost (close to the lower bound of the 99% confidence interval equal to that for the as polished specimens at the same chloride concentration and temperature, as shown in Figure 3.

To verify that E_{rp} is as a threshold potential for the occurrence of localized corrosion of Zr-4, a potentiostatic test was conducted using a mechanically polished specimen in J-13 simulated well water containing 1.0 M NaCl at 95 °C and an applied potential of 0.055 V_{SCE}. This potential represents an overpotential of approximately 15 mV with respect to the E_{rp} value calculated from Eq.(2) for the same chloride concentration. Upon the application of the potentiostatic step from the E_{corr}, the current density increased initially and then decayed to a steady state value of 0.75 mA/cm^2. Extensive attack was observed on the specimen surface outside the area defined by the crevice former after only 3 min of polarization.

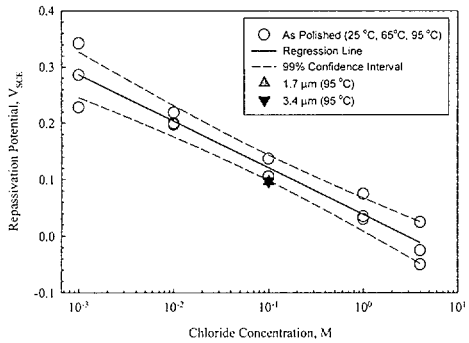

Figure 3. Repassivation potentials as a function of chloride concentration for mechanically polished specimens of Zircaloy-4 in simulated J-13 well water compared to values obtained for specimens covered with a hydrothermally grown oxide

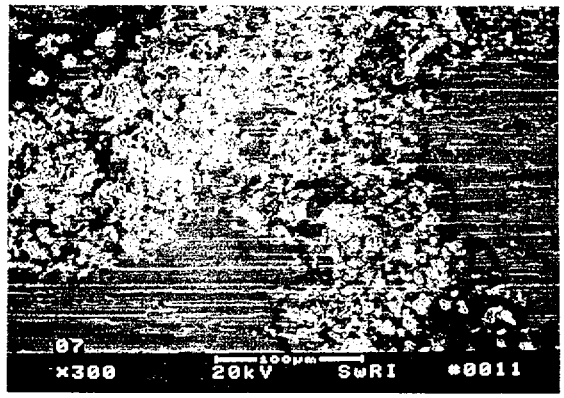

Figure 4. SEM micrograph showing typical pitting morphology observed after anodic potentiostatic polarization of polished specimen of Zircaloy-4 in deaerated 1M NaCl solution at 95 °C and at potentials above E_{rp}

The typical morphology of the localized corrosion of polished Zr-4 specimens exposed to chloride-containing simulated J-13 water at 95 °C is shown in Figure 4. The attack was found to be irregularly distributed over the boldly exposed specimen surface and occurred mostly beneath the oxide layer displaying a shallow and irregularly shaped network of oxide covered pits. As noted previously[6], no detectable localized attack was observed under the crevice former, despite that this occluded geometry represents the most aggressive environmental condition for many passive metals and alloys.[5] However, in the hydrothermally oxidized (non-creviced) specimens the attack was confined to more localized areas but still partially covered by the oxide, as shown at a lower magnification in Figure 5. As revealed in a cross sectional view of the specimen (Figure 6), the attack penetrated deep into the metal, apparently along some preferential orientations, leaving behind a highly porous mass of black corrosion products. The spongy appearance of the corrosion products is clearly noticeable in Figure 7. X-ray diffraction was used to identify the major components of the black corrosion products easily extracted as a powder from the attacked area. As shown in Figure 8, the major components were identified as metallic Zr and a zirconium hydride ($ZrH_{0.25}$) with only traces of a zirconium oxychloride ($ZrOCl_2 \cdot 6H_2O$), whereas zirconium oxide (ZrO_2) was found to be present in a minor proportion.

Figure 9 shows the values of E_{rp} for as polished specimens in 0.1 M chloride solution at 95 °C with the addition of 0.0005 and 0.010 M NaF. It is clearly shown in Figure 9 that the measured values lie within the 99 percent confidence interval for the lineal logarithmic plot of E_{rp} as a function of the chloride concentration for the simulated J-13 well water in which the NaF concentration is only 0.0001 M. Also, a E_{rp} value of 0.1 V_{SCE}, which is almost identical to that measured for the polished specimens, was obtained in 0.1 M chloride solution at 95 °C with the addition of both 0.0005 and 0.010 M NaF using specimens covered with an oxide film hydrothermally grown for 2 weeks at 300 °C.

The effect of the hydrothermally grown oxide film thickness on the initiation time for pitting corrosion under potentiostatic conditions is displayed in Figure 10. This figure shows plots of the anodic current density as a function of time in 0.1 M NaCl solution at 95 °C and an applied potential of 0.125 V_{SCE} for specimens covered with oxide films grown in water at 300 °C from 2 to 12 weeks (see Table 2) as compared to the plot for a polished specimen. It is clearly illustrated in Figure 10 that at a potential that is only 15 to 25 mV above E_{rp} the initiation time for pitting corrosion, as indicated by the abrupt jump in current density from a very low value, increased significantly with oxide film thickness. Pit initiation eventually occurred, but more than 40 days were required to induce pitting corrosion in the specimen with the thickest oxide compared to few minutes for the polished specimen. Even though it is not evident as a result of the scale used in Figure 10, the current density measured before passivity breakdown was about 10^{-8} A/cm^2 and almost independent of oxide film thickness, with the single exception of the specimen with an oxide film grown for 8 weeks at 300 °C, which exhibited pronounced current fluctuations from the beginning of the potentiostatic test.

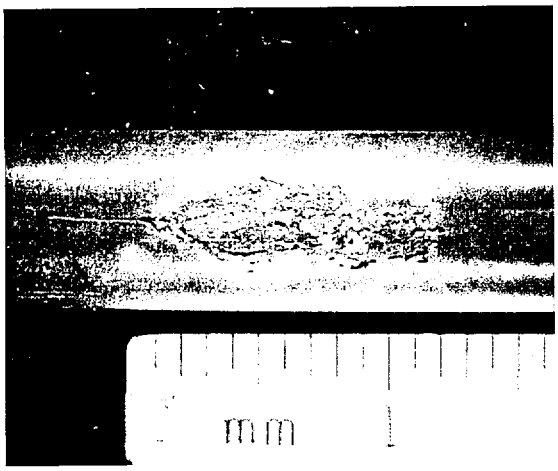

Figure 5. Low magnification photograph showing the typical morphology of the localized corrosion observed after anodic potentiostatic polarization of Zircaloy-4 specimen covered with a hydrothermally grown oxide film in chloride containing solutions at potentials above E_{rp}

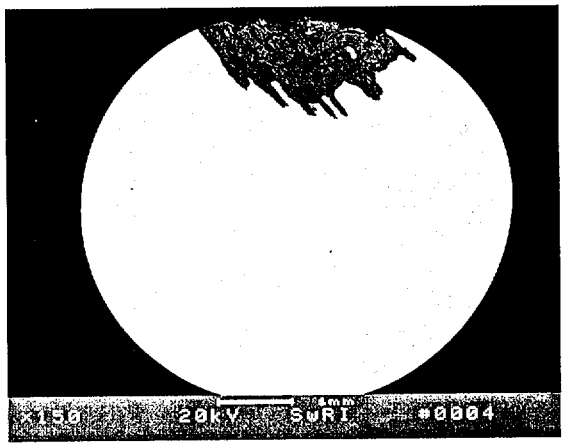

Figure 6. SEM micrograph showing a cross sectional view of the localized corrosion observed after anodic potentiostatic polarization of Zircaloy-4 specimen covered with a hydrothermally grown oxide film in chloride containing solutions at potentials above E_{rp}

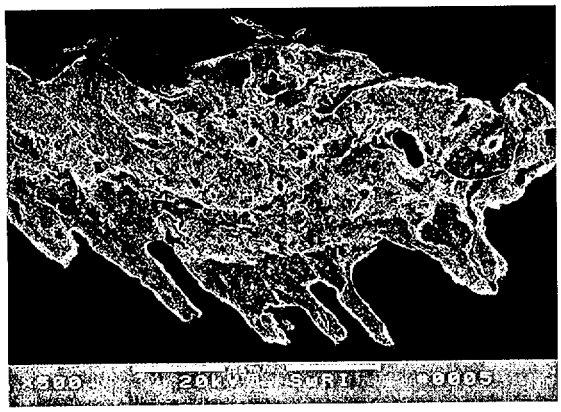

Figure 7. SEM micrograph showing a more detailed view of the localized corrosion and the appearance of the corrosion products observed after anodic potentiostatic polarization of Zircaloy-4 specimen covered with a hydrothermally grown oxide film in chloride containing solutions at potentials above E_{rp}

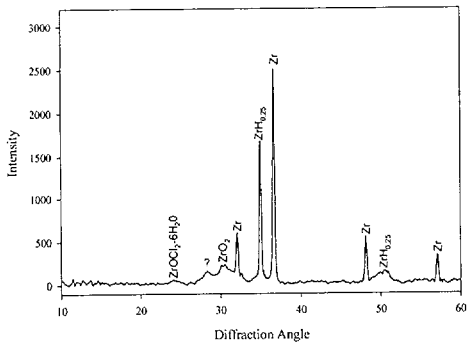

Figure 8. X-ray spectrum of the corrosion products found in a pit of Zircaloy-4 showing, in addition to the Zr peaks, the assignment of the high intensity peak to $ZrH_{0.25}$

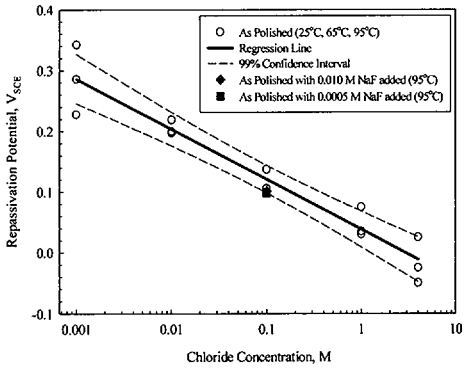

Figure 9.Repassivation potentials as a function of chloride concentration for mechanically polished specimens of Zircaloy-4 in simulated J-13 well water compared to values obtained with the addition of 0.0005 and 0.010 M NaF to 0.1 M NaCl solution at 95 °C

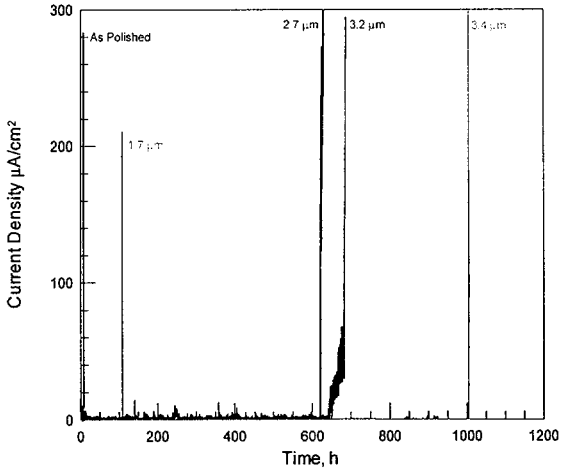

Figure 10. Anodic current density as a function of time for mechanically polished and oxide covered specimens of Zircaloy-4 with various film thicknesses in 0.1 M NaCl solution at 95 °C under an applied potential of 0.125 V_{SCE}

Plots of the evolution of E_{corr} of Zr-4 in air saturated 0.1 M NaCl at 95 °C, before and after the addition of H_2O_2 or $FeCl_3$ (attaining a concentration of 5 mM), are shown in Figure 11. Specimens covered with an oxide film hydrothermally grown at 300 °C for 2 and 8 weeks were used in these tests. There are no clear trends in the evolution of E_{corr} during the initial 150 hours of exposure. Specimens with a 2-week oxide film exhibited an initial decay in E_{corr} followed by an increase, with a constant difference of approximately 300 mV between the values of E_{corr} for the two specimens. For the specimens with the thicker oxide film the difference between the values of E_{corr} was larger, approximately 450 mV, but the potential increased initially, reached a peak, and increased again after a minor decay. As expected, the E_{corr} values were found to be higher in average for the specimens with the thicker oxide film. After the addition of H_2O_2, however, the values of E_{corr} became similar (< 100 mV difference) regardless of the oxide film thickness, reaching at the end of the test values close to those measured initially in the air saturated solution without H_2O_2. On the other hand, E_{corr} values increased with the addition of $FeCl_3$ became higher, and remained relatively constant for the duration of the test. However, no pitting corrosion initiation was observed after approximately 840 hours (~35 days) on the specimens exposed under open circuit potential conditions to the chloride solution after the addition of $FeCl_3$ even though the E_{corr} values (differing in ~300 mV for these two specimens with different oxide thickness) were higher than E_{rp}. In the chloride solution containing H_2O_2 the E_{corr} values were close to E_{rp}, and pitting corrosion was not initiated, suggesting that a certain over potential is needed to promote pitting vapor open circuit conditions.

Discussion

As shown in Figure 3, E_{rp} for Zr-4 exhibits a linear dependence on the logarithm of the chloride concentration that extends from concentrations of the order of mM to values close to NaCl saturation. As noted,[6] the slope of this dependence, represented by B in Eq. (2), is approximately equal to 0.083 V/decade, a value similar to that reported by Maguire[8] for commercially pure Zr and slightly higher than the theoretical value derived by Galvele in his model of pitting corrosion.[9] The data shown in Figure 3 indicate that both B and E^{o}_{rp} are independent of temperature practically up to the boiling point of water. This observation confirms that Zr-4, contrary to the case of many metals and alloys,[5,10] does not exhibit a decrease in E_{rp} and E^{o}_{rp} with increasing temperature in the range of 25 to 95 °C. As also shown in Figure 3, the presence of an oxide film with thickness estimated to range from 1.7 to 3.2 μm (see Table 2) does not affect the value of E_{rp}.

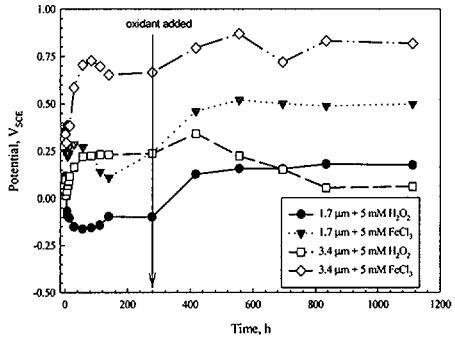

Figure 11. Effect of H_2O_2 and $FeCl_3$ additions on the open circuit potential of Zr-4 specimens, covered with hydrothermally grown oxide films of different thickness, in air saturated 0.1M NaCl solution at 95 °C

On the contrary, as shown in Figures 1 and 2, E_b was found to be more than 500 mV higher in the case of the specimens covered with the hydrothermally grown oxide layers. No such significant influence of the oxide film was previously observed[6] in the case of specimens covered with a oxide layer formed in air at 200 °C for 8 weeks in which the thickness was estimated to be about 154 nm. It is apparent that a thicker oxide affects significantly the pit initiation process and this delayed initiation provides an explanation for the high E_b value measured by scanning the potential in a potentiodynamic polarization test. This interpretation is confirmed by the results plotted in Figure 10. As indicated by the abrupt current rise, the pit initiation time at potentials just above E_{rp} increased significantly with increasing oxide layer thickness. It took about 42 days to initiate pitting corrosion when the oxide layer was about 3.4 μm thick. These results suggest that in the presence of thicker oxide films, such as those formed on spent nuclear fuel cladding, extremely long testing times may be required to initiate localized corrosion of Zircaloy. Hence, if sufficient time is allowed for pit initiation to occur, the difference between E_b and E_{rp} tends to become negligible but justifies the use of E_{rp} as a useful threshold parameter that can be determined in a short- term electrochemical for predicting the occurrence of localized corrosion.[11] On the contrary, E_b, determined from CPP testing, as many times has been reported,[5] is not as useful a parameter because it is dominated by the random nature of the pit initiation process and therefore extremely dependent on experimental factors, such as surface preparation and roughness, potential scan rate, passivation times, and other test conditions.

It should be noted, in relation to the role of the thick preformed oxide layer that the morphology of the localized attack changed substantially, as shown by comparing figures 4 through 7. It appears that deeper pits can only develop as a result of the better protection offered to the surrounding surface by the thermally grown film, contrary to the case of the thin passive films formed after mechanical polishing in low temperatures (< 100 °C) aqueous solutions or air which are only about 4 to 6 nm thick.[4]

Another important observation is the presence of metallic Zr and $ZrH_{0.25}$ as the main corrosion products inside pits. There are two possible alternative explanations for this observation. As observed by Postlethwaite and Onofrei,[12] it appears that anodic disintegration occurred during pitting corrosion forming, in addition to a gel of $Zr(OH)_4$, a metal powder (α-Zr) that can react with water generating H_2 gas (and eventually $ZrH_{0.25}$). The other explanation is that H^+ ions, generated by hydrolysis of Zr^{4+} ions produced by active dissolution in the pit, are reduced to atomic hydrogen that immediately formed $ZrH_{0.25}$ by reaction with the metal. In this second case, however, the presence of Zr as a metallic powder cannot be easily justified.

As the chloride concentration in the solution increased to values close to the solubility of NaCl, E_{rp} decreased to near 0.0 $V_{SCE,}$ as shown in figure 3. Although not confirmed in this study at such high concentrations, a similar behavior can be expected for specimens covered with a thick oxide layer This indicates that localized corrosion of Zr-4 is likely to occur under disposal conditions if this range of chloride concentration is attained in the presence of oxidizing species such as radiolysis products or reducible cationic species (i.e., Fe^{3+}) arising from the corrosion of carbon steel baskets used inside WPs to maintain fuel assembly positions. It is not known if these conditions, in terms of availability of reducible species at a sufficiently high concentration, are likely to occur in the environment in contact with the Zr-4 spent fuel cladding in the proposed repository. If this is the case, the possibility of localized corrosion needs to be evaluated further.

As noted in Figure 11 the addition of $FeCl_3$ increases E_{corr} above E_{rp} and can lead to the initiation of localized corrosion. However, it appears also from the results presented in Figure 11, that pitting corrosion is not easily initiated under open circuit conditions at least within the duration of these tests (42 days). One possibility is that the current supplied by

the cathodic reduction of Fe^{3+} to Fe^{2+} ions (plus that resulting from the O_2 reduction) is not sufficient to promote pit initiation and growth because the ZrO_2 is a poor electronic conductor. Although the intermetallic particles existing in Zr-4 [1,13] constitute a potential electronic conduction path, the path might be interrupted because the particles remained embedded and isolated in an oxide layer of sufficient thickness. In addition, Fe^{3+} cations might not be available in sufficiently high concentrations in the experiment. This may be a possible situation inside containers because, if the pH of the waste package internal environment is buffered by the presence of relatively high concentrations of HCO_3^- anions, precipitation of ferric oxyhydroxides may occur, decreasing the concentration of free Fe^{3+} cations.

An additional effect to consider relates to the role of hydrogen peroxide. It is assumed that reducible species generated by the radiolysis of water may increase the E_{corr} observed in air-saturated solutions above E_{rp}. In addition to unstable radicals, hydrogen peroxide is the most stable molecular species generated by water radiolysis. However, hydrogen peroxide seems to act as a mild oxidant in the presence of a thick oxide layer, as shown in figure 11. This observation is contrary to the effect previously reported in the presence of thinner (~150 nm) oxide films.[6]

An additional factor that may inhibit the occurrence of pitting corrosion is the effect of other anions present in the ground water. According to a review of the literature,[4] the strength of the inhibiting effect of these anions decreases in the order: $NO_3^- > SO_4^{2-} > HCO_3^-$. It was previously discussed,[6] however, that the ratio of the sum of the weighted concentration of inhibitor anions (X^-_i) to chloride ion concentration is the important parameter to evaluate the inhibiting efficiency. Inhibition only occurs when this ratio is far greater than one.

Additional work is necessary to evaluate the effect of these anions taking into consideration the range of concentrations that can be attained in the aqueous environment in contact with breached waste packages. On the other side, additions up to 0.01 M of F^-, which is the remaining major anion present in the groundwater, did not influence the E_{rp} values measured in simulated J-13 well water, as shown in figure 9. The results were similar regardless of the use of polished or oxide covered specimens. Nevertheless, it should be expected that at higher concentrations, and particularly under mild acidic conditions, F^- anions may destabilize the ZrO_2 passive film.[4]

The results of our studies[6] have confirmed that Zr-4 is more resistant to crevice corrosion than to pitting corrosion, contrary to the case of many corrosion resistant alloys such as stainless steels and Ni-Cr-Mo alloys in which the passive behavior is related to the presence of a Cr-rich passive film. The preferential occurrence of pitting corrosion on boldly exposed surfaces, rather than in the tight crevice existing on the specimens, can be explained because Zr does not exhibit an active loop even in concentrated HCl solutions as stainless steels and Ni-base alloys. As a consequence, the metal surface inside the crevice region remains passive without the localized depassivation usually caused by the simultaneous action of high concentrations of H^+ and Cl^- ions. In this regard Zr is very similar to Ta, which also exhibits resistance to crevice corrosion and lacks an active loop in strong acid solutions. No simple explanation exists for this behavior and additional studies are required. Finally, it should be clearly stated that at potentials lower than E_{rp}, even in the presence of highly concentrated and acidified chloride solutions, Zr-4 is extremely resistant to corrosion as a result of the protection offered by a very stable and passive ZrO_2 film. In this range of potentials, steady state current densities much lower than 1×10^{-8} A/cm^2 ($<< 0.1\mu$m/yr) have been measured.[4]

Conclusions

- Zircaloy-4, either mechanically polished or covered with a hydrothermally grown oxide layer, is susceptible to pitting corrosion in chloride-containing solutions at concentrations above 0.001M and potentials higher than a repassivation potential which depends linearly on the logarithm of the chloride concentration but is temperature independent.

- No crevice corrosion is observed under the same environmental and electrochemical conditions that promote pitting corrosion.

- Although the presence of a hydrothermally grown oxide film does not affect the value of the repassivation potential, it promotes a significant increase in the corrosion potential in air-saturated $FeCl_3$-containing solutions.

- The corrosion potential can reach the repassivation potential in $FeCl_3$-containing solutions and therefore pitting corrosion of Zircaloy 4 fuel cladding may occur under natural corroding conditions inside a breached container, but additional studies on the kinetics of the cathodic reactions on oxide covered surfaces are needed to predict the long-term performance of cladding as an additional metallic barrier to radionuclide release in the disposal of spent nuclear fuel.

Acknowledgments

This investigation was conducted with the support of Nuclear Regulatory Commission under Contract No. NRC-02-97-009. The paper presents the opinions of the authors and in no way is intended to reflect or represent the views or regulatory position of the US Nuclear Regulatory Commission. The technical assistance provided by S. Clay and B. Derby (Southwest Research Institute) are gratefully appreciated.

References

1. U.S. Department of Energy, "Yucca Mountain Science and Engineering Report," DOE/RW–0539, 2001.

2. B. Cox, Advances in Corrosion Science and Technology, 5 (1976): pp. 173–391.

3. B. Cox, "Degradation of Zirconium Alloys in Water Cooled Reactors," Third International Symposium on Environmental Degradation of Materials in Nuclear Power Systems—Water Reactors (Warrendale, PA: The Metallurgical Society, 1988), pp. 65–76.

4. G.A. Cragnolino, D.S. Dunn, C.S. Brossia, V. Jain, and K.S. Chan, "Assessment of Performance Issues Related to Alternate Engineered Barrier System Materials and Design Options," CNWRA 99-003, 1999.

5. Z. Szklarska-Smialowska, "Pitting Corrosion of Metals" (Houston, TX: National Association of Corrosion Engineers, 1986).

6. C.A. Greene, C.S. Brossia, D.S. Dunn, and G.A. Cragnolino, "Environmental and Electrochemical Factors on the Localized Corrosion of Zircaloy-4," CORROSION/2000, paper no. 210 (Houston, TX: NACE International, 2000).

7. E. Hillner, D.G. Franklin, and J.D. Smee, "The Corrosion of Zircaloy-Clad Fuel Assemblies In a Geologic Repository Environment," WAPD–T–3173, 1994.

8. M. Maguire, "The Pitting Susceptibility of Zirconium in Aqueous Cl^-, Br^-, and I^- Solutions," Industrial Applications of Titanium and Zirconium: Third Conference, ASM STP 830 (Philadelphia, PA: American Society for Testing and Materials, 1984): pp. 175–189.

9. J.R. Galvele, Journal of the Electrochemical Society 123 (1976): pp. 464–474.

10. G.A. Cragnolino, "A Review of Pitting Corrosion in High-Temperature Aqueous Solutions," Advances in Localized Corrosion (Houston, TX: National Association of Corrosion Engineers, 1990): pp. 413–431.

11. D.S. Dunn, N. Sridhar, and G.A. Cragnolino, Corrosion 52 (1996): pp. 115–124.

12. J. Postlethwaite and M. Onofrei, Corrosion 35 (1979): pp. 185–189.

13. J.B. Van der Sande and A.L. Bement, Journal of Nuclear Materials 52 (1974):115–118.